

**Photobiomodulation therapy drives massive epigenetic histone modifications, stem cells mobilization, and accelerated epithelial healing**

Manoela D. Martins, DDS, PhD<sup>1,3,6</sup>, Felipe Martins Silveira<sup>3</sup>, MSc, Marco A. T. Martins DDS, PhD<sup>1,4</sup>, Luciana O. Almeida, PhD<sup>5</sup>, Vanderlei S. Bagnato<sup>2</sup>, Cristiane H. Squarize DDS, PhD<sup>6</sup>, Rogerio M. Castilho DDS, PhD<sup>6\*</sup>

<sup>1</sup> Department of Oral Pathology, School of Dentistry, Federal University of Rio Grande do Sul, Rio Grande do Sul, Brazil.

<sup>2</sup> São Carlos Institute of Physics, University of São Paulo (USP), São Carlos, São Paulo, Brazil.

<sup>3</sup> Department of Oral Diagnosis, Piracicaba Dental School, University of Campinas, Piracicaba, Brazil.

<sup>4</sup> Department of Oral Medicine, Hospital de Clínicas de Porto Alegre (HCPA/UFRGS), Federal University of Rio Grande do Sul, Porto Alegre, Rio Grande do Sul, Brazil.

<sup>5</sup> Laboratory of Tissue Culture, Department of Basic and Oral Biology, University of Sao Paulo School of Dentistry, Ribeirao Preto, Brazil.

<sup>6</sup> Laboratory of Epithelial Biology, Department of Periodontics and Oral Medicine, University of Michigan School of Dentistry, Ann Arbor, MI, USA.

\*Corresponding author:

Rogerio M. Castilho, DDS, MS, PhD

Laboratory of Epithelial Biology

Department of Periodontics and Oral Medicine

University of Michigan

1011 N University Ave, Room 2029C

Ann Arbor, MI, 48109-1078

Phone: (734) 647-2150

e-mail: [rcastilh@umich.edu](mailto:rcastilh@umich.edu)

This is the author manuscript accepted for publication and has undergone full peer review but has not been through the copyediting, typesetting, pagination and proofreading process, which may lead to differences between this version and the Version of Record. Please cite this article as doi: [10.1002/jbio.202000274](https://doi.org/10.1002/jbio.202000274)

**Data Sharing:** The data that support the findings of this study are available from the corresponding author upon reasonable request.

**Abstract**

Emerging evidence indicates the clinical benefits of photobiomodulation therapy (PBMT) in the management of skin and mucosal wounds. Here we decided to explore the effects of different regimens of PBMT on epithelial cells and stem cells, and the potential implications over the epigenetic circuitry during healing. Scratch-wound migration, immunofluorescence (anti-acetyl-Histone H3, anti-acetyl-CBP/p300, and anti-BMI1), nuclear morphometry, and western blotting (anti-Phospho-S6, anti-MBD2) were performed. Epithelial stem cells were identified by the aldehyde dehydrogenase enzymatic levels and sphere-forming assay. We observed that PBMT induced accelerated epithelial migration and chromatin relaxation along with increased levels of histones acetylation, the transcription co-factors CBP/p300, and mTOR. We further observed a reduction of the transcription repression-associated protein MBD2 and a reduced number of epithelial stem cells and spheres. In this study, we showed that PBMT could induce epigenetic modifications of epithelial cells and control stem cell fate, leading to an accelerated healing phenotype.

**Keywords:** Photobiomodulation; Low-Level Laser Therapy; Histone acetylation; Epigenetics; Wound healing.

## Introduction

Wound healing is a dynamic process that coordinates cellular events essential for tissue repair and the reestablishment of the epithelial barrier function [1]. The healing process consists of three main overlapping phases: the inflammatory phase, followed by cellular proliferation, and the tissue remodeling phases [2]. During the proliferative phase, keratinocytes undergo proliferation followed by migration and ultimately undergo differentiation and stratification [3]. When considering the importance of the wound healing process in the maintenance of tissue homeostasis, the speed by which epithelial cells close the wound is key in the reduction of water loss and in the mitigation of infections. There are multiple therapeutic approaches currently in use in the clinic that facilitate tissue healing. Among them, the use of antibiotics, anti-inflammatory drugs, herbal medicines, surgical debridement of necrotic tissues in case of burn wounds, and, more recently, the application of photobiomodulation therapy (PBMT) to improve healing [4,5].

The PBMT is defined as the application of nonionizing forms of light such as lasers, light-emitting diodes, and broadband light to promote physiological changes and therapeutic benefits [6]. PBMT has been considered an important tool in accelerating wound healing in both experimental [7,8] and clinical settings [9,10]. Most studies have used different sources of laser light, and the benefits in tissue healing are related to the effects of laser irradiation directly to the cells. PBMT triggers cellular biostimulation via the excitation of intracellular chromophores such as mitochondrial and membrane cytochromes, endogenous porphyrins, and flavoproteins [11]. Nonetheless, the effects of PBMT on tissues are dependent on the irradiation along with the treatment parameters that include wavelength, output power, exposure time, and irradiated area [12]. Despite the positive results demonstrated by PBMT in epithelial cells [13-15], a number of variables, including

the application parameters and the optimal dose, remain unknown, and the molecular mechanisms involved in the stimuli of epithelial tissues and its stem cells. There are already some studies identifying different mechanisms of action of PBMT in irradiated tissues, such as the activation of TGF- $\beta$ 1 and mTOR signaling, and the modification of histone acetylation and NF $\kappa$ B expression [10,16,17]. However, the effects of PBMT therapy on epigenetic modifications of epithelial cells and its potential implication over stem cell maintenance remain poorly understood.

Epigenetics refers to the study of changes in gene expression without the alteration of the nucleotide sequence of the genetic code [18]. Epigenetic modifications include DNA methylation, histone modifications, and noncoding RNA, also known as microRNAs [19]. Covalent modifications in the histone tails directly influence the chromatin organization and the DNA packaging. More specifically, histone acetylation on the residue of lysine 9 in the tail of histone H3 (H3K9ac) is considered an epigenetic marker for active chromatin. Increased acetylation levels of H3K9ac result in relaxed chromatin, increased binding of transcription factors, and significantly increased gene expression. These epigenetic mechanisms promote dynamic alterations in the cell transcriptional potential and regulate many biological processes, including cell proliferation, migration and differentiation, signaling pathway activation or inhibition, and cell senescence. During wound healing, the involvement of epigenetic processes like the loss of the polycomb group proteins and the methylation of histones has been described in specific developing stages of injured tissues [1]. The activation of selective genes at very particular moments determines the phases of cell proliferation, differentiation, and migration.

Although there is a body of data stating the importance of PBMT in the process of wound healing, the effects of laser irradiation on epigenetic mechanisms of reepithelization and in the modulation of stem cells are not yet totally elucidated. In this sense, our study aimed to evaluate the impact of different PBMT protocols on the behavior and epigenetic modifications of epithelial cells and stem cells.

## Materials and Methods

### *Cell Lineages and Materials*

Keratinocyte cell line (HaCaT) was cultured in Dulbecco's modified Eagle's medium (DMEM) supplemented with 10% fetal bovine serum (FBS), 100 U/ml penicillin, 100 µg/ml streptomycin, and 250 ng/ml amphotericin B. The cells were maintained in a 5% CO<sub>2</sub>-humidified incubator at 37°C.

Cells were seeded on tissue culture plates and cultured until achieving 70% of cellular confluency. Cells were cultured until 100% of confluency exclusively during wound assay. Cell stress was induced by culturing cells with a low concentration of FBS (DMEM with 2% FBS, nutritional deficit) [20,21]. The laminar flow (biosafety class II) was used to perform all the cell culture experiments, and cells were monitored daily using a phase-contrast microscope (Nikon Eclipse Ts2, Nikon, Melville, New York).

### *Photobiomodulation Therapy (PBMT)*

All laser irradiations were executed using continuous wave indium–gallium–aluminum–phosphide (InGaAlP, 660nm) diode laser (Twin Laser, MM Optics, Sao Paulo, Brazil) in a punctual mode with a spot size of 0.04cm<sup>2</sup>). Five groups with different PBMT parameters were established using different output power (40mW and 100mW) and energy densities (4J/cm<sup>2</sup> and 20J/cm<sup>2</sup>) (Table 1). All laser application was carried out at a 90° angle in relation to the tissue-culture plates. The sham control group was manipulated identically to the treatment conditions omitting the laser irradiation (laser off). Each culture condition was seeded in a different culture dish to avoid exposure of cells due to cross-irradiation. The laser therapy was administered in close contact with the base of the optically clear plates to maintain

optimal irradiation. The process of cellular irradiation was conducted under partially dark conditions to avoid the potential interference of other light sources. The output power of the laser was continuously monitored using a power meter (Laser Check; MM Optics LTDA, Sao Paulo, Brazil).

### ***Scratch-wound migration assay***

The ability of epithelial cells to migrate upon different parameters of PBMT irradiations was assessed using an *in vitro* scratch-induced wound model. Keratinocytes were seeded on 60mm culture plates and kept at 37°C with FBS supplement until complete cellular confluence. The culture medium was replaced by a nutritional-deficient media (2% FBS) in all groups two hours before the scratch, as previously described [13,20]. Two perpendicular crossing scratches (lines) were performed in the center of the confluent monolayer of epithelial cells utilizing a 200µl pipette tip (Figure 1A). After scratch, time zero was established and used as the baseline for all future measurements. We applied four irradiations sessions with 6h of intervals between each procedure. Each 60mm culture plates received five distinct irradiation points (Figure 1A) [20]. The first irradiation timepoint followed the scratching (T0). In order to standardize and guide the irradiation time points, circles were drawn at the bottom of each culture dish using a permanent marker, as illustrated in Figure 1A. Wound closure was assessed and photographed at 0, 12h, 24h, 48h, 60h, 72h, 84h, and 96h time points using an inverted microscope. Wound closure was mensurated by using software to analyze the images, and the percentage of the closed area was calculated (AxioVision 4.8.1, Carl Zeiss, New York). All scratch assays were conducted in replicate with an analysis of 8 areas in each group.

### ***Immunofluorescence and Nuclear Size Analyzes***

Keratinocytes cells were seeded on glass coverslips in individual 60mm

culture plates and maintained for 12h at 37°C with normal growth. The culture media was replaced by nutritional-deficit media in all groups (0% FBS). After 48h of starving condition, each coverslip was exposed to three cycles of PBMT irradiation respecting intervals of 6h (0, 6h, and 12h) with different parameters, as described in Table 1. After the last PBMT session, cells were fixed with absolute methanol at -20°C for 5 min, followed by immunofluorescence staining. Briefly, Triton X-100, 0.5% (v/v) in PBS, was used to block cells in combination with 3% (w/v) bovine serum albumin following incubation with anti-acetyl-histone H3 (acH3 Lys9, 1:100) and anti-acetyl-CBP (Lys1535)/p300 (Lys 1499, 1:100) both antibodies from Cell Signaling Technology, Danvers, Massachusetts. After a wash in PBS (3x), cells were incubated with Alexa 488 (green) and 546 (red)-conjugated secondary antibodies and stained with Hoechst 33342 (DAPI) for visualization of DNA content.

Images of 10 fields of each group were captured at 400x magnification using a QImaging ExiAqua monochrome digital camera attached to a Nikon Eclipse 80i microscope (Nikon, Melville, New York) and visualized with QCapturePro7 software, as previously described [22]. Grayscale images were captured separately after fluorescence excitation using FITC\_HYQ and TRITC\_HYQ filters. Cells receiving 300nM of the histone deacetylase inhibitor Trichostatin A (TSA) diluted in media for 24h were used as positive controls for histone acetylation. CBP/p300 morphometric analyses were performed using the ImageJ (Version 1.38s; NIH, Bethesda, MD). For nuclear evaluation, 50 cells of each group stained with DAPI were measured using ImageJ software.

### ***Western Blotting***

Keratinocyte cells were seeded into 60mm culture plates and maintained for 12h at 37°C in a humidified incubator with 5% CO<sub>2</sub> in culture media supplemented with 10% FBS. The culture media was substituted by nutritional-deficit media in all groups (2% FBS). After 48h of starving condition, each PBMT group received three



sessions of PBMT irradiations with 6h intervals (0, 6h, and 12h) with different parameters, as described in Table 1. At the end of the last PBMT session, the cells were washed with cold PBS and lysed with RIPA buffer. After centrifugation at 4°C for 10 min, protein lysates were loaded and run in 10% SDS-PAGE gels and transferred to polyvinyl difluoride membrane (Millipore, Billerica, Massachusetts). After protein transfer, the membranes were blocked with 5% milk solution for 1hr following washed with TBS-Tween and incubated overnight with anti-methyl-CpG binding domain protein 2 (MBD2) (Bethyl Laboratories, Montgomery, Texas, 1:2000), anti-phospho S6 (Cell Signaling, Danvers, Massachusetts, 1:2000), and GAPDH as a loading control (Calbiochem, Gibbstown, New Jersey). The membranes were washed (3x) with TBS-Tween followed by the incubation of the secondary antibodies conjugated with horseradish peroxidase for 1hr at room temperature (RT). The reactions were visualized using the ECL Super Signal West Pico Substrate (Pierce Biotechnology, Rockford, Illinois). Optical density (OD) of representative WB bands were quantified using ImageJ. OD of MBD2 and pS6 proteins were normalized to the corresponding OD for the same well for GAPDH to control for small changes in protein loading.

### *Sphere assay*

To evaluate the impact of PBMT over epithelial stem cells,  $2.5 \times 10^3$  keratinocytes were cultured in ultra-low attachment plates to generate spheres (Corning; New York, NY, USA). After five days of growth, culture media was substituted by nutritional-deficit media in all groups (2% FBS). Then, two groups were established: the Sham group (without irradiation) and the PBMT group. Epithelial spheres received the same PBMT protocol described in Table 1. The PBMT group received three sessions of irradiations with 6h intervals during four consecutive days. The sham group received identical treatment conditions omitting the laser irradiation. Cytospin was applied at 1500 rpm, 4°C for 10 min, and the slides were stained with hematoxylin-eosin (H&E) or submitted to immunofluorescence for

detection of acetyl-histone H3 (ac.H3 Lys9, 1:100, Cell Signaling), B-cell-specific Moloney murine leukemia virus integration site 1 (BMI1, cloneF6, 1:50, Millipore) and acetyl-CBP (Lys1535)/p300, 1:100, Cell Signaling). The total number of spheres was counted in 100x magnification using a Nikon Eclipse 80i microscope (Nikon, Melville, New York).

### ***Fluorescence-Activated Cell Sorting (FACS) of Epithelial Stem Cells***

Aldehyde dehydrogenase (ALDH) activity (Aldefluor kit, StemCell Technologies, Durham, NC, USA) assay was used to identify epithelial stem cell-like cells using flow cytometry. Briefly,  $5 \times 10^4$  keratinocytes were plated in 60mm culture plates and maintained for 12h at 37°C in a humidified chamber maintained at 5% CO<sub>2</sub> concentration in DMEM supplemented with 10% FBS. The culture media was substituted by nutritional-deficit media in all groups (2% FBS). Two groups were established: Sham (without irradiation) and PBMT. The PBMT group received three sessions of irradiations with 6h intervals during four consecutive days using the same protocol described in Table 1. The cells were suspended with activated Aldefluor substrate (BODIPY-amino acetate) or negative control (diethylaminobenzaldehyde, a specific ALDH inhibitor) for 45 minutes at 37°C. Ten thousand events were counted for each sample using the FACSDiVA Cell Sorter (BD Biosciences, Mountain View, CA, USA).

### ***Statistical Analysis***

All statistical analyses were performed using GraphPad Prism (GraphPad Software, San Diego, California). Two-way ANOVA statistical analysis was applied in the scratch assay and western blot assay, followed by Tukey's multiple comparison tests. Nuclear size measure, acH3, and CBP/p300 stains statistical analyses were performed using a one-way analysis of variance and Tukey's multiple comparison tests. Asterisks denote statistical significance (\* p<0.05, \*\* p<0.01, \*\*\* p<0.001,

\*\*\*\* p<0.0001 and ns p>0.05).

## Results

### ***PBMT accelerated epithelial wound healing independent of the irradiation parameters***

Here we decided to explore if distinctive PBMT parameters would produce a different effect on epithelial migration. Using a scratch wound healing approach and keratinocyte cells, we observed that all PBMT parameters resulted in accelerated epithelial migration.

Overall, we observed that the application of 40mW output produced a superior result over the epithelial cells when compared to 100mW (Fig. 1B and C). Cells exposed to 40mW started to migrate faster than the sham group by 12 hours, while cells receiving 100mW shown accelerated migration by 24h after irradiation (Fig. 1C). Consistent with the early start in cellular migration, keratinocytes completely closed the scratch wound after 60 hours when receiving 40mW of output. Cells receiving 100mW, however, only achieved complete closure by 72h after wound (Fig. 1C). The sham group exhibited closure within 84h and 96h after wound.

### ***PBMT induced chromatin remodeling associated with epigenetic modification and activation of mTOR (mammalian target of rapamycin) pathway in epithelial cells***

Following, we decided to evaluate if PBMT was able to induce morphological changes to epithelial cells. Interestingly, we observed that irradiated cells respond to PBMT by increasing the nuclear size independent of the output power and the energy density used (Fig. 2A).

Chromatin decompaction is a sign of epigenetic modifications. With that in mind, we decided to explore the effects of low power irradiation on histone acetylation. We observed that both energy densities (4J/cm<sup>2</sup> and 20J/cm<sup>2</sup>) resulted in

increased acetylation levels of histone H3 at lysine 9 (H3K9ac) independent of the output power used (40mW or 100mW) (Fig. 2B). We further decided to explore if PBMT would also have an effect on transcriptional co-activating proteins, therefore, suggesting a mechanism for histone modifications. Indeed, we observed that PBMT is capable of triggering the expression of the transcription co-factors CBP and p300 (Fig. 2C). We further decided to explore if MBD2, a protein involved in the recognition of methylated CpG islands and therefore associated with gene transcription repression, would be affected by PBMT. Western blot of irradiated keratinocyte lysates demonstrated that administration of low energy densities (4J/cm<sup>2</sup> and 20J/cm<sup>2</sup>) diminished the protein levels of MBD2, in special at 20J/cm<sup>2</sup> and output power of 100mW (Fig. 2D). We have previously shown that PBMT influences the expression levels of the mTOR signaling pathway. We observed that PBMT induces upregulation of the mTOR pathway by the activation of pS6 in keratinocytes independent from the output power used (40mW or 100mW) (Fig. 2E).

#### ***PBMT promoted modification in keratinocytes stem cells***

We have previously shown that changes in the chromatin organization have a profound impact on the population of cancer cells and cancer stem cells [23,24], however little is known on the ability of PBMT in modulating normal epithelial stem cells. Here we found that PBMT has a significant impact on the number of ALDH positive cells when compared to sham (\* $p < 0.05$ ) (Fig. 3A). Increased enzymatic activity of ALDH is a strong indication of cells presenting enriched stem and progenitor function. Along with the detection of ALDH enzymatic levels, we also explored the impact of PBMT on epithelial spheres. Epithelial cells cultured in low adhesion conditions form spheres presenting enrichment for stem cells. We found a reduction in the total number of spheres in PBMT groups (\*\* $p < 0.01$ ) (Fig. 3B). Further characterization of irradiated epithelial spheres indicates a relative accumulation of H3K9ac, CBP/p-300, and BMI-1 compared with sham controls (Fig. 3C).

## Discussion

The effects of PBMT on tissue repair are well documented in a broad range of studies [15,25,26]. While some mechanisms of action associated with PBMT were described in the literature, little is known about the relation of PBMT with epigenetic and stem cells [17,27]. The activation and differentiation of stem cells have an important role in the restorative capacity of the wound healing process [28,29]. Our study demonstrates for the first time that while PBMT accelerates epithelial migration, it promotes chromatin remodeling and mobilizes the population of stem cells. Here, we investigate the ability of PBMT to stimulate keratinocyte migration and accelerate epithelial wound healing using different parameters. We observed that the lower power output of 40mW provided faster effects than using 100mW (Fig. 1). Indeed, we previously demonstrated augmented epithelial migration and accelerated wound healing of keratinocytes with 40mW (4 and 20J/cm<sup>2</sup>) [13]. Nonetheless, the use of higher output power of 100mW was also shown to be effective in accelerating healing. In this sense, it was previously demonstrated that the power density seems to influence cell growth in an inversely proportional manner [30]. PBMT has shown biostimulatory effects, such as faster epithelial cell migration [13] and proliferation [8,20], which are important events in the wound healing process. Therefore, PBMT appears very useful in the clinic setting as it accelerates the healing process of different oral mucosal disorders, such as oral mucositis, oral lichen planus, recurrent aphthous stomatitis, and herpes infection [31-35].

The ability of PBMT to induce epigenetic chromatin modifications shown here is exciting and demonstrates that low power laser is capable of modulating gene expression in epithelial cells. Indeed, some of the effects of laser irradiation on chromatin properties were previously described in the study of Smol'yaninova et al. [36]. In this study, irradiated (He-Ne laser, 632.8nm, 28-11J/m<sup>2</sup>) human peripheral blood lymphocytes presented chromatin activation potentially related to a more responsive behavior of these cells to natural stimulators present in tissues. In this context, the authors concluded that this effect might help to explain the mechanism of wound healing following irradiation. Interestingly, in the present study, PBMT

promoted nuclear modification similar or superior to TSA, an HDAC inhibitor capable of inducing broad chromatin acetylation. TSA selectively inhibits HDAC classes I and II, inducing histone modifications while preventing the deacetylation of histone lysine [37]. The acetylation of lysine residues of histones and the recruiting of protein histone acetyltransferases (HATs) are often associated with transcriptionally active genes [37,38]. Indeed, the use of PBMT in epithelial cells resulted in the acetylation of H3K9ac along with the nuclear accumulation of CBP/p300. CBP/p300 has an important function associated with chromatin remodeling, and it is a transcriptional coactivator factor that plays distinct roles, such as bridging of DNA-binding and general transcription factors and relaxation of chromatin through its intrinsic HATs activity [39]. Interestingly, HATs can also interact and acetylate other substrates besides histones. Although CBP/p300 does not directly acetylate H3K9, it interacts with several transcription factors to regulate gene expression, such as ATF2, E2F, NFkB, and HMG protein [40,41] and CBP/p300 also acetylates and activates non-histone proteins, like the tumor suppressor p53 [42]. These characteristics indicate the importance of CBP/p300 in the regulation of many physiological processes, including cell growth, transformation, development, and apoptosis [43].

Our findings, therefore, provide evidence that PBMT promotes epithelium wound healing associated with epithelial migration and epigenetic modifications, such as increases in H3K9 acetylation and CBP/p300. Several epigenetic mechanisms have been shown to be engaged in regulating epithelial homeostasis and wound repair [44,45]. Antagonism of histone deacetylases (HDAC) using HDAC inhibitor valproic acid promoting acetylation of histones has been shown to improve tissue regeneration, including the spinal cord of mice [46]. In addition, induction of Histone H3 and H4 acetylation promoted by the administration of valproic acid also activates AKT/mTOR pathway, increasing the levels of Rictor, Raptor, pS6, and Akt, suggesting a link between mTOR and the epigenetic machinery in prostate cancer cells [47]. In an animal that undergone digital amputation, the administration of intraperitoneal injections of HDAC inhibitor presented increased proliferation and

collagen deposition at the amputation site, leading to improved digital regeneration compared with controls [48]. In this study, PBMT presented similar behavior to HDACi, promoting chromatin remodeling and histone acetylation. In an animal model of oral tongue ulcer healing, our group demonstrated that PBMT induces epithelial migration during the initial stages of healing along with enhanced keratinocyte differentiation at the late stage of healing. Such a process involved the acetylation of histones and the expression of NFkB [17].

Epigenetic regulation comprises the interaction between histone modifications and DNA methylation through the association of proteins at specific sites of the DNA [49]. MBD proteins coordinate the signaling between cytosine methylation and chromatin structure, acting as transcriptional regulators. Interestingly, MBD2, a member of MBD proteins, recruits the Nucleosome Remodeling and Deacetylase (NuRD) co-repressor complex and repress transcription through the methylation of CpG islands of the associated genes [49]. In this study, it was observed that laser irradiation with the energy densities used resulted in diminished levels of MBD2, which was more evident for 20J/cm<sup>2</sup> using an output power of 100mW. The reduced levels of MBD2 associated with the accumulation of H3K9ac and CBP/p300 suggest that PBMT induces an epigenetic reprogramming responsible for activating gene transcription while downregulating MBD2 and its ability to repress gene transcription. Among all of these processes, our group has been focused on identifying signaling pathways associated with the effects of PBMT-induced epithelial cell migration. Among several pathways, we have identified the PI3K/mTOR signaling as a major player in the process of epithelial reepithelialization [13]. Here, we decided to verify if the epigenetic modification induced by PBMT was associated with enhanced epithelial migration.

The oral epithelium is an actively renewable tissue presenting a reservoir of stem cells localized at the basal layer. Epithelial stem cells represent a minor population of cells with a strong capability to self-renew, to maintain tissue homeostasis, and to repair damaged tissues [50]. Different stimuli, including PBMT,

can induce stem cells to proliferate and activate terminal differentiation. To analyze the effects of PBMT in keratinocyte stem cells, we explored the effects of low power laser over ALDH levels, a known detoxifying enzyme involved in the oxidation of intracellular aldehydes [51]. ALDH may have a function in the early differentiation of stem cells through its role in oxidizing retinol to retinoic acid being considered a functional marker for the stem cell population. High ALDH levels have been reported in stem cells from different tissues and to be present at high levels in cancer stem [52,53]. Following the administration of PBMT, we observed a significant reduction of ALDH<sup>+</sup> cells when compared to the sham. Parallel to the use of ALDH levels to identify stem cells, we decided to implement a functional assay to enrich stem cells by inducing the formation of spheres. Upon administration of PBMT, we observed a reduction in the total number of spheres when compared to the sham-treated spheres. Combined, ALDH and sphere-forming assays demonstrate that PBMT promotes a reduction in the total number of epithelial stem cells.

In addition, to verify the effect of PBMT in the expression of epigenetic markers in the stem cell population, it was performed an immunofluorescence labeling in the spheres. The results showed an increase in H3K9ac and CBP/p-300 expression after PBMT, indicating that diode laser promoted chromatin remodeling in keratinocyte stem cells. There is growing evidence that epigenetic alteration may cause specific chromatin changes to distinguish stem and differentiated cells in a wide range of tissues [54]. Histone acetylation has been described as a regulator of differentiation and self-renewal of multiple types of stem [55]. However, the role of histone acetylation in differentiation depends on the specific cell type and phase of development.

The differentiation process indicates that pluripotent stem cells give rise to specialized cells. While differentiating, cells undergo several stages of cellular differentiation and progressively specialized at each step. However, the mechanism associated with the stem cell's decision to self-renew or differentiate still needs to be completely elucidated. A handful of molecular markers involved in this stem cell conundrum have been identified, including the BMI1. While BMI1 is observed in



stem cells, its overexpression reduces apoptosis and increases cellular proliferation in mesenchymal stem cells [56]. Such a process involves the repression of p16INK4 and prevents stem cells from undergoing cellular senescence. Indeed, we observed that low power laser induces the accumulation of BMI1 in the epithelial spheres. We also observed that laser therapy also reduced the number of spheres being formed. The remainder spheres are characterized by higher levels of BMI1, suggesting the potential role in the stem cell decision to self-renew or differentiate.

Collectively, our results indicated that PBMT stimulates a pronounced effect on the organization of chromatin in epithelial cells causing relaxation in its configuration around the bound DNA sequences by acetylation of histones, activation of CBP/p300, and reduction of MBD2, leading to an increase in nuclear size. Histone acetylation and CBP/p300 activation have been described as important signaling endpoints involved in cellular plasticity in both normal and tumoral cells, regulating the expression of genes involved in various biological mechanisms, such as cell proliferation, differentiation, and survival. The present study is the first one to demonstrate that PBMT can modulate the epigenetic signature of keratinocytes and its stem cell population, which may justify some of the important effects previously attributed to PBMT, such as cellular proliferation, cellular migration, and reestablishment of the cellular metabolism.

## **Acknowledgments**

This work was funded by the NIH – NIGMS (PIs: Drs. Squarize and Castilho – R01GM120056). This work was entirely performed at the laboratory of Epithelial Biology at the University of Michigan. The funder had no role in study design, data collection, and analysis, decision to publish, or preparation of the manuscript. The authors have no other relevant affiliations or financial involvement with any organization or entity with a financial interest in or financial conflict with the subject matter or materials discussed in the manuscript apart from those disclosed. Drs. Martins and Bagnato were funded by CAPES - Finance Code 001, FAPERGS n.17/0045-5, and FAPESP n. 2013/07276-1 (for scholarship and fellowship).

## **Conflict of Interest**

The authors declare that there are no conflicts of interest.

## **Author contributions**

MD Martins, MAT Martins, CH Squarize, and RM Castilho contributed equally in the design of the study, acquisition, analysis, and interpretation of data, writing the manuscript, revising it critically, approving the final version to be published, and agreeing to be accountable for all aspects of the work. FM Silveira, LO Almeida, and VS Bagnato contributed equally in the analysis and interpretation of data, writing the manuscript, revising it critically, approving the final version to be published, and agreeing to be accountable for all aspects of the work.

## References

- [1] T. Shaw and P. Martin. EMBO reports, **2009**, 10, 881.
- [2] T. Velnar, T. Bailey, V. Smrkolj. J Int Med Res, **2009**, 37, 1528.
- [3] R. M. Castilho, C. H. Squarize, C. H. Gutkind. Oral Dis, **2013**, 19, 551.
- [4] V. P. Wagner, L. Meurer, M. A. Martins, C. K. Danilevicz, A. S. Magnusson, M. M. Marques, M. S. Filho, C. H. Squarize, M. D. Martins. J Biomed Opt, **2013**, 18, 128002.
- [5] K. Nuutila, J. Grolman, L. Yang, M. Broomhead, S. Lipsitz, A. Onderdonk, D. Mooney, E. Eriksson. Adv Wound Care, **2020**, 9, 48.
- [6] J. Anders, P. R. Arany, G. D. Baxter, R. J. Lanzafame. Photobiomodul Photomed Laser Surg, **2019**, 37, 63.
- [7] P. V. Peplow, T. Y. Chung, G. D. Baxter. Photomed Laser Surg, **2012**, 30, 118.
- [8] F. G. Basso, C. F. Oliveira, C. Kurachi, J. Hebling, C. A. S. Costa. Lasers Med Sci, **2013**, 28, 367.
- [9] D. G. Minatel, M. A. C. Frade, S. C França, C. S. Enwemeka. Lasers Surg Med, **2009**, 41, 433.
- [10] M. A. T. Martins, M. D. Martins, C. A. Lascala, M. M. Curi, C. A. Migliorati, C. A. Tennis, M. M Marques. Oral Oncol, **2012**, 48, 79.
- [11] R. Ankri, R. Lubart, R. Taitelbaum. Lasers Surg Med, **2010**, 42, 760.

- [12] V. P. Wagner, L. Meurer, M. A. T. Martins, C. K. Danilevicz, A. S. Magnusson, M. M. Marques, M. S. Filho, C. H. Squarize, M. D. Martins. *J Biomed Opt*, **2013**, 18, 128002.
- [13] A. C. A. Pellicoli, M. D. Martins, C. S. Dillenburg, M. M. Marques, C. H. Squarize, R. M. Castilho. *J Biomed Opt*, **2014** 19, 028002.
- [14] I. Khan, P. R. Arany. *Photomed Laser Surg*, **2016**, 34, 550.
- [15] P. M. Tricarico, L. Zupin, G. Ottaviani, S. Pacor, F. Jean-Louis, M. Boniotto, S. Crovella. *J Biophotonics*, **2018**, 11, e201800174.
- [16] P. R. Arany, A. Cho, T. D. Hunt, G. Sidhu, K. Shin, E. Hahm, G. X. Huang, J. Weaver, A. C. Chen, B. L. Padwa, M. R. Hamblin, M. H. Barcellos-Hoff, A. B. Kulkarni, D. J. Mooney. *Sci Transl Med*, **2014**, 6, 238ra69.
- [17] A. F. Gabriel, V. P. Wagner , C. Correa, L. P. Webber, E. F. S. Pilar, M. Curra, V. C. Carrard, M. A. T. Martins, M. D. Martins. *Lasers Med Sci*, **2019**, 34, 1465.
- [18] S. L. Berger, T. Kouzarides, R. Shiekhattar, A. Shilatifard. *Genes Dev*, **2009**, 23, 781.
- [19] M. Ducasse, M. A. Brown. *Mol Cancer*, **2006**, 5, 60.
- [20] F. P. Eduardo, D. U. Mehnert, T. A. Monezi, D. M. Zezell, M. M. Schubert, C. P. Eduardo, M. M. Marques. *Lasers Surg Med*, **2007**, 39, 365.

- [21] L. Almeida-Lopes, J. Rigau, R. A. Zângaro, J. Guidugli-Neto, M. M. Jaeger. *Lasers Surg Med*, **2001**, 29, 179.
- [22] F. S. Giudice, D. S. Pinto Jr, J. E. Nör, C. H. Squarize, R. M. Castilho. *PLoS One*, **2013**, 8, e58672.
- [23] V. P. Wagner, M. D. Martins, R. M. Castilho. *Methods Mol Biol*, **2018**, 1692, 179.
- [24] L. P. Webber, V. Q. Yujra, P. A. Vargas, M. D. Martins, C. H. Squarize, R. M. Castilho. *Cancer Lett*, **2019**, 461, 10.
- [25] R. C. Mosca, A. A. Ong, O. Albasha, K. Bass, P. Arany. *Adv Skin Woun Care*, **2019**, 32, 157.
- [26] M. Bagheri, A. Mostafavinia, M. Abdollahifar, A. Amini, S. K. Ghoreishi, S. Chien, M. R. Hamblin, S. Bayat, M. Bayat. *Biomedicine Pharmacother*, **2020**, 123, 109776.
- [27] A. Amaroli, S. Ravera, F. Baldini, S. Benedicenti, I. Panfoli, L. Vergani. *Lasers Med Sci*, **2019**, 34, 495.
- [28] R. M. Castilho, C. H. Squarize, K. Leelahavanichkul, Y. Zheng, T. Bugge, J. S. Gutkind. *PloS one*, **2010**, 5, e10503.
- [29] A. R. Z. Zamani, S. Saberianpour, M. H. Geranmayeh, F. Bani, L. Haghghi, R. Rahbarghazi. *Lasers Med Sci*, **2020**, 35, 299.

- [30] L.H. Azevedo, F. de Paula Eduardo, M. S. Moreira, C. de Paula Eduardo, M. M. Marques. *Lasers Med Sci*, **2006**, 21, 86.
- [31] S. A. Al-Maweri, B. Kalakonda, N.A. AlAizari, W. Al-Soneidar, S. Ashraf, S. Abdulrab, E. S. Al-Mawri. *Lasers Med Sci*, **2018**, 33,1423.
- [32] J. Amorim Dos Santos, A. G. C. Normando, I. P. de Toledo, G. Melo, G. De Luca Canto, A. R. Santos-Silva, E. N. S. Guerra. *Clin Oral Investig*, **2020**, 24, 37.
- [33] C. S. Dillenburg, M. A. T. Martins, M. C. Munerato, M. M. Marques, V. C. Carrard, M. S. Filho, R. M. Castilho, M. D. Martins. *J Biome Opt*, **2014**, 19, 068002.
- [34] J. C. Spanemberg, M. A. Z. Figueiredo, K. Cherubini, F. G. Salum. *Altern Ther Health Med*, **2016**, 22, 24.
- [35] J. Zecha, J. Raber-Durlacher, R. Nair, J. Epstein, S. Elad, M. Hamblin 7, A. Barasch, C. Migliorati, D. Milstein, M. Genot, L. Lansaat, R. Brink, J. Arnabat-Dominguez, L. Molen, I. Jacobi, J. Diessen, J. Lange, L. Smeele, M. Schubert, R. Bensadoun. *Support Care Cancer*, **2016**, 24, 2793.
- [36] N. K. Smol'yaninova, T. I. Karu, G. E. Fedoseeva, A. V. Zelenin AV. *Biomed Sci*, **1991**, 2, 121.
- [37] M. D. Martins, R. M. Castilho. *J Carcinog Mutagen*, **2013** 1, 1.
- [38] C. E. Brown, T. Lechner, L. Howe, J. L. Workman. *Trends Biochem Sci*, **2000**, 25, 15.

- [39] P. A. Wade, D. Pruss, A. P. Wolffe. Trends Biochemical Sci, **1997**, 22, 128.
- [40] L. Morris, K. Allen, N. La Thangue. Nat Cell Biol, **2000**, 2, 232.
- [41] H. Chan, N. La Thangue. J Cell Sci, **2001**, 114, 2363.
- [42] N. Shikama, C. W. Lee, S. France, L. Delavaine, J. Lyon, M. Krstic-Demonacos, N. B. La Thangue. Mol cell, **1999**, 4, 365.
- [43] R. Goodman, S. Smolik. Genes Dev, **2000**, 14, 1553.
- [44] T. Odorisio. J Invest Dermatol, **2016**, 136, 738.
- [45] L. Rouhana, J. Tasaki. Stem Cells Int, **2016**, 2016, 6947395.
- [46] L. Lv, Y. Sun, X. Han, C. Xu, Y. Tang, Q. Dong. Brain Res, **2011**, 1396, 60.
- [47] J. Makarević, N. Tawanaie, E. Juengel, M. Reiter, J. Mani, I. Tsaour, G. Bartsch, A. Haferkamp, R. A. Blaheta. J Cell Mol, **2014**, 18, 1460.
- [48] G. Wang, S. F. Badylak, E. Heber-Katz, S. J. Braunhut, L. Regen Med, **2010**, 5, 201.
- [49] M. A. Desai, H. D. Webb, L. M. Sinanan, J. Scarsdale, N. Walavalkar, G. D. Ginder, D. C. Williams Jr. Nucleic Acids Res, **2015**, 43, 3100.

[50] B. Calenic, M. Greabu, C. Caruntu, C. Tanase, M. Battino. *Periodontol* 2000, **2015**, 69, 68.

[51] G. Duester. *Eur J Biochem*, **2000**, 267, 4315.

[52] L. O. Almeida, D. M. Guimarães, C. H. Squarize, R. M. Castilho. *Cancers*, **2016**, 4, 8, 78.

[53] D. Guimarães, L. Almeida, M. Martins, K. Warner, A. Silva, P. Vargas, F. Nunes, C. Squarize, J. Nör, R. Castilho. *Oncotarget*, **2016**, 7, 42447.

[54] M. Frye, A. Fisher, F. Watt. *PloS one*, **2007** 2, e763.

[55] Y. Qiao, R. Wang, X. Yang, K. Tang, N. Jing. *J Biol Chem*, **2015**, 290, 9949.

[56] Y. Jung, J. Nolte. *Curr Stem Cell Res Ther*, **2016**, 11, 131-140.



## Figure legends

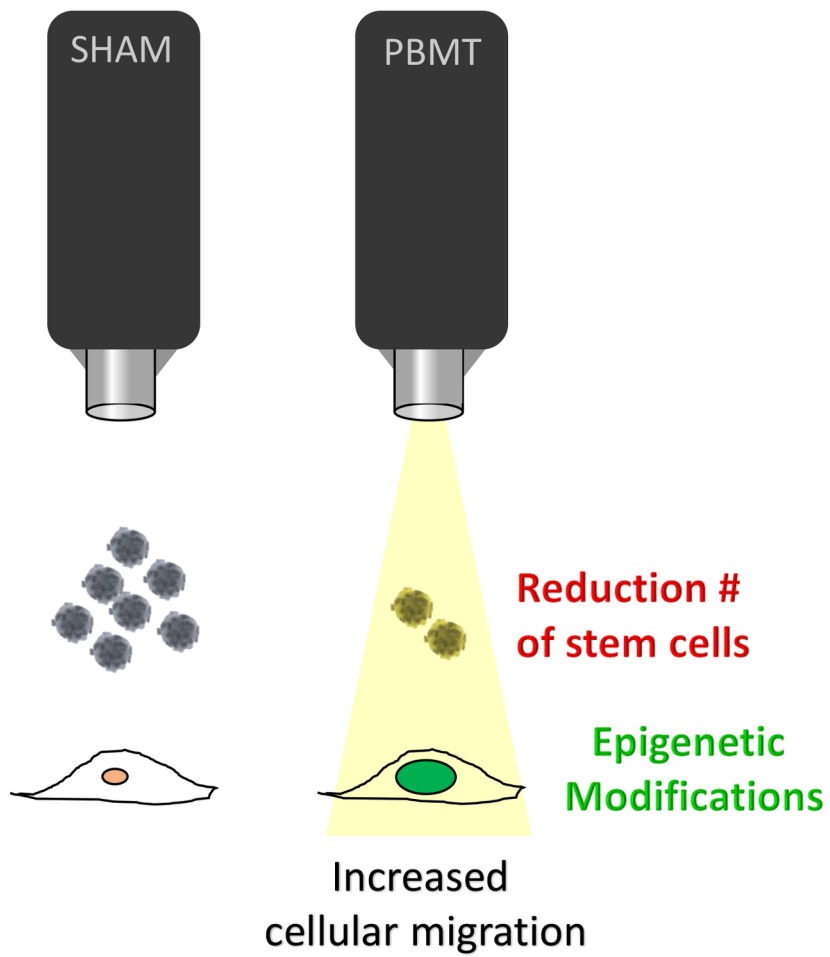
**Figure 1.** Scratch-wound migration assay. (A) Illustration of the irradiated area following the orientation points marked on the bottom of each culture dish well. Representation of the photographed areas within each scratch-wound assay. (B and C) PBMT accelerated keratinocyte migration. In the first 12h, only the PBMT groups with 40mW output power showed a significant acceleration of migration compared to control. At 24h and 48h time points, all the PBMT groups receiving 40mW and 100mW of output power demonstrated accelerated wound healing (\*  $p < 0.05$ ).

**Figure 2.** PBMT induced chromatin remodeling and epigenetic modification in epithelial cells. (A) Significant increase in the nuclear size of keratinocyte in all PBMT groups compared with baseline control and TSA-treated cells (positive control). (B) PBMT induces chromatin remodeling evident by increased levels of H3K9ac, and (C) accumulation of CBP/p300 in keratinocytes. (D and E) Representative Western blots of MBD2c and pS6 after PBMT treatment of keratinocytes. Optical density (OD) of representative WB bands were quantified using ImageJ. OD of MBD2 and pS6 proteins were normalized to the corresponding OD for the same well for GAPDH to control for small changes in protein loading (\*\*\*\*  $p < 0.0001$ ; \*\*\*  $p < 0.001$ ; \*\*  $p < 0.01$ ).

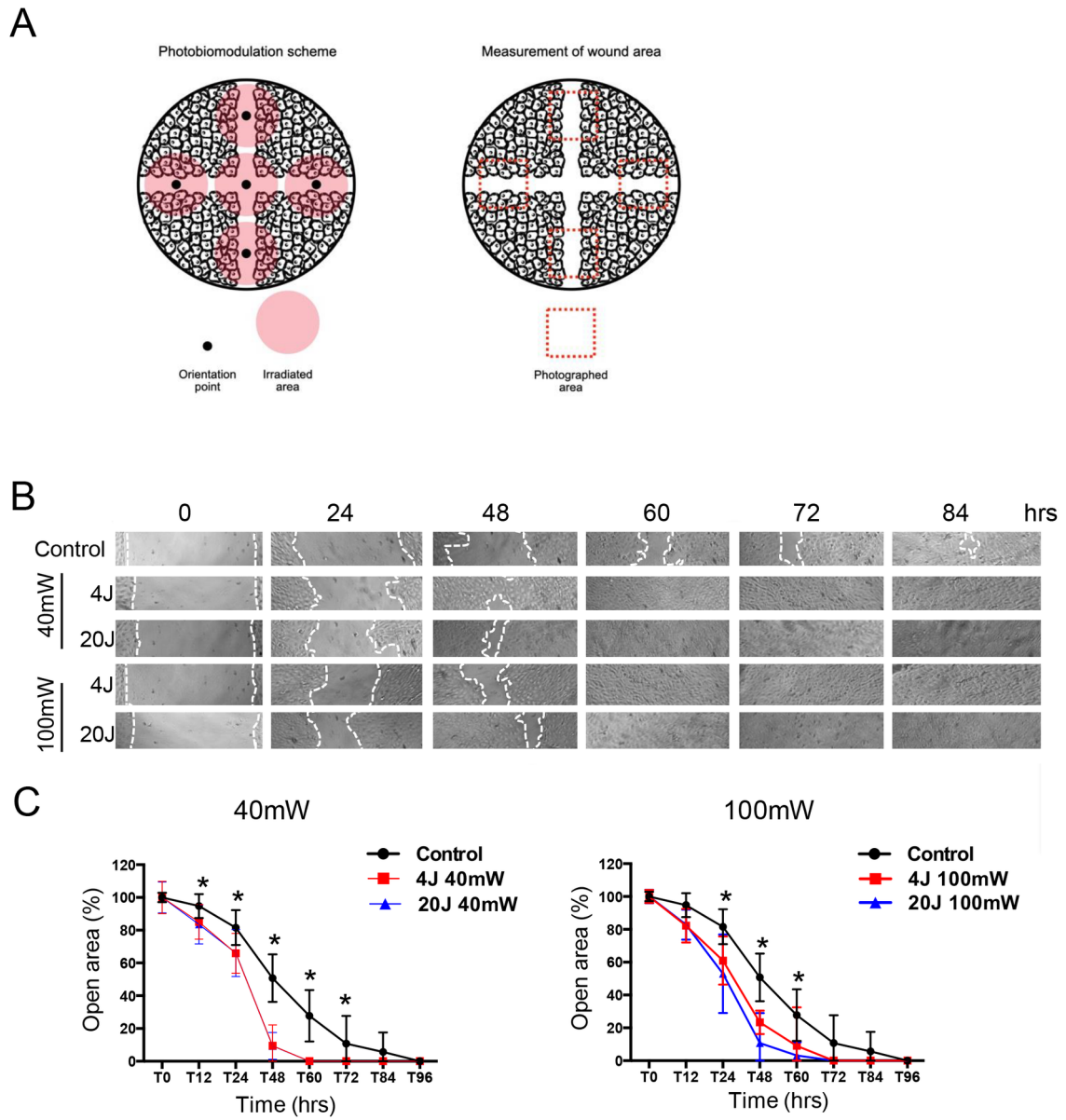
**Figure 3.** Stem cell analysis. (A) PBMT caused a reduction in ALDH<sup>+</sup> cells and (B) in the total number of epithelial spheres. (C) Keratinocyte spheres demonstrated an increase in H3K9ac, CBP/p-300, and BMI-1 after PBMT (\*  $p < 0.05$ ; \*\*  $p > 0.01$ ).

Emerging evidence indicates the clinical benefits of photobiomodulation therapy (PBMT) in the management of skin and mucosal wounds. Here we explored the effects of different regimens of PBMT on epithelial cells and stem cells, and the potential implications over the epigenetic circuitry during healing. We observed that PBMT induced accelerated epithelial migration and chromatin relaxation along with increased levels of histones acetylation. We showed that PBMT could induce epigenetic modifications of epithelial cells and control stem cell fate, leading to an accelerated healing phenotype.

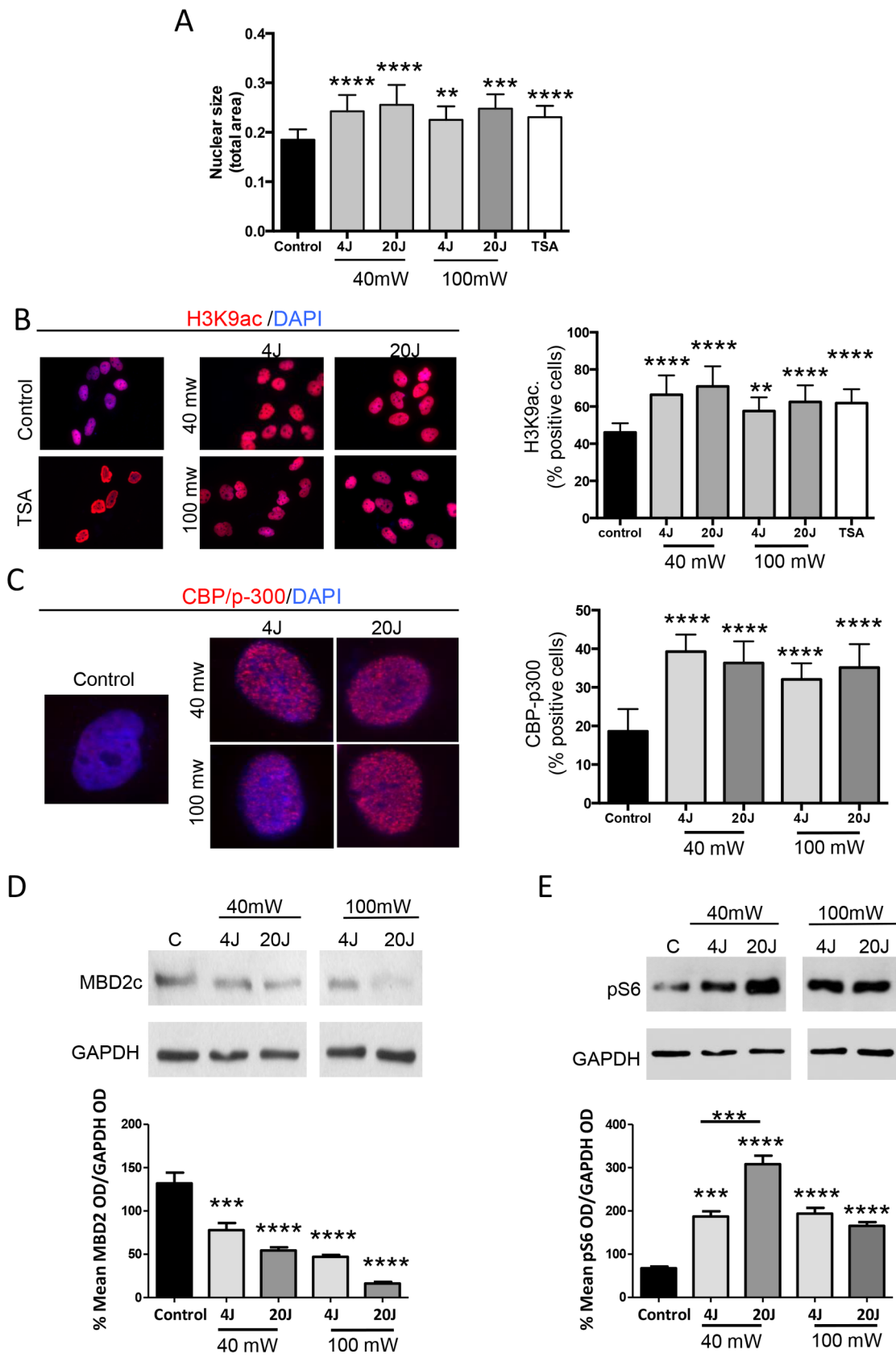
Photobiomodulation therapy triggers epigenetic modifications



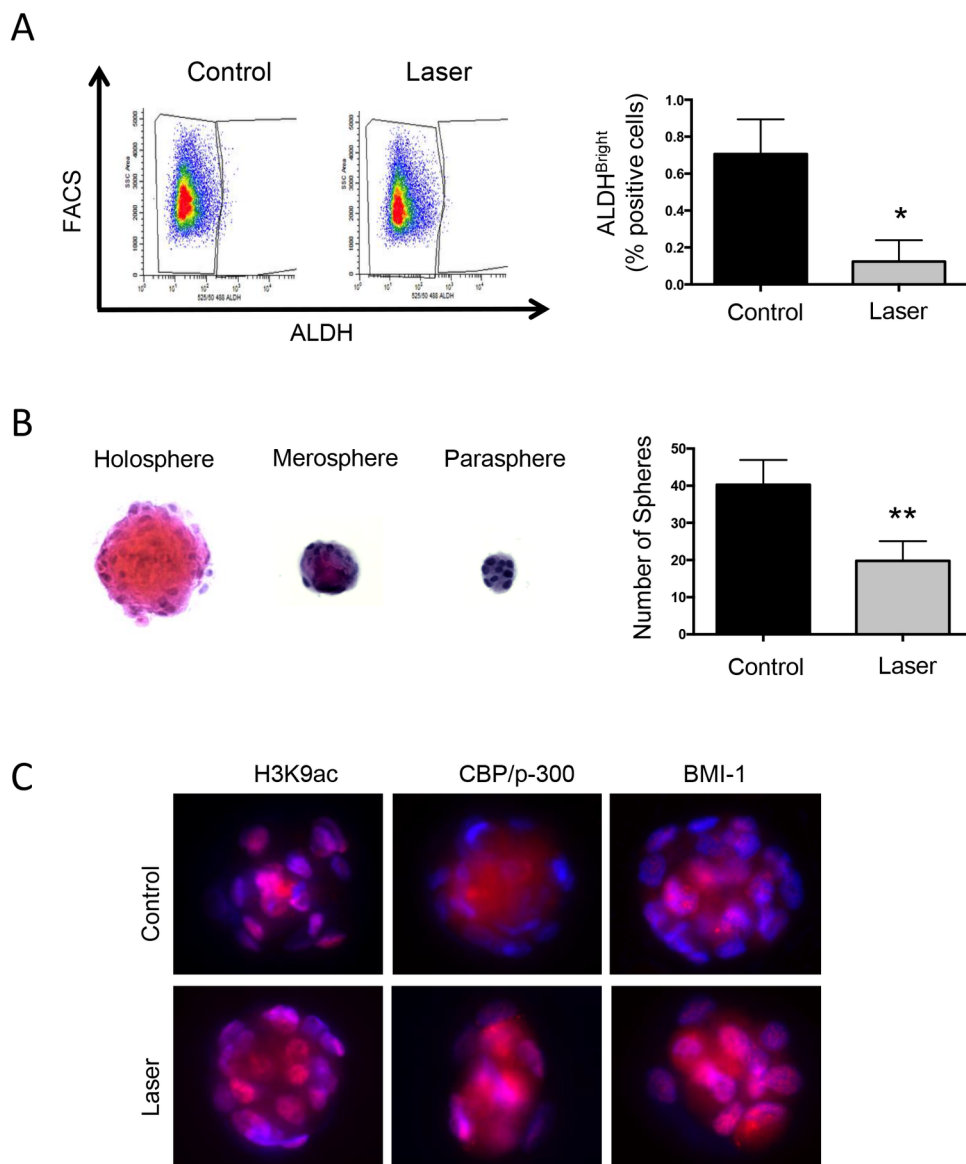
JBIO\_202000274\_Graphical abstract v3.tif



JBIO\_202000274\_Martins et al figure 1 Resubmission.tif



JBIO\_202000274\_Martins et al figure 2 Resubmission.tif



JBIO\_202000274\_Martins et al figure 3 Resubmission.tif

**Table 1.** Photobiomodulation therapy parameters used.

	Wavelength (nm)	Power (mW/cm <sup>2</sup> )	Energy Density (J/cm <sup>2</sup> )	Irradiation time (s)	Energy (J)
SHAM	0	0	0	0	0
Group 1	660	40	4	4	0.16
Group 2	660	40	20	20	0.8
Group 3	660	100	4	1.6	0.16
Group 4	660	100	20	8	0.8